Journal of Radioanalytical and Nuclear Chemistry (2020) 326:87–96
https://doi.org/10.1007/s10967-020-07288-1

Development of mesoporous γ-alumina from aluminium foil waste for ^{99}Mo/^{99m}Tc generator

Miftakul Munir[1] · Sriyono[1] · Abidin[1] · Endang Sarmini[1] · Indra Saptiama[1] · Kadarisman[1] · Marlina[1]

Received: 24 January 2020 / Published online: 23 July 2020

Abstract
Mesoporous alumina (MA) has been produced from aluminium foil waste, and its performance as a sorbent in a ^{99}Mo/^{99m}Tc generator has been evaluated. The resulting MA demonstrated excellent properties with the specific surface area of 209.8 m^2 g^{-1} and Mo adsorption capacity of 60.2 ± 1.5 mg g^{-1}. It was able to release ^{99m}Tc with a high yield percentage and to comply with the required standard. Our successful effort on the synthesis of aluminium foil based alumina sorbent has opened the possibility of further work on the development of waste-based alumina for separation.

Keywords Alumina · Molybdenum-99 · Technetium-99 · Radionuclide generator

Introduction

Technetium-99m (^{99m}Tc) is the most widely used radionuclide for diagnostic purposes in nuclear medicine with more than 30 million applications annually. ^{99m}Tc is derived from its parent radionuclide, molybdenum-99 (^{99}Mo), and available in a radionuclide generator [1]. ^{99}Mo is routinely produced from uranium-235 (^{235}U) using research reactors generating high specific activity ^{99}Mo. Alumina with Mo adsorption capacity of 20 mg g^{-1} is sufficient as a column filler, which adsorbs ^{99}Mo. After 24 h, adsorbed ^{99}Mo will decay to ^{99m}Tc and able to be eluted using a saline solution. ^{99m}Tc in saline solution can be used for labelling of various radiopharmaceutical kits intended for a diagnosis of diseases, such as cancers, infections and organ disorders [2].

The ^{99}Mo supply worldwide is supported by a few research reactors using ^{235}U. This supply is vulnerable proved by the ^{99}Mo shortage in 2009 as two reactors shut down for repairs and maintenances purposes. The possibility of a ^{99}Mo shortage in the future due to ageing of the research reactors urges scientists around the world to find alternative ways of ^{99}Mo production. There are several potential production routes for maintaining ^{99}Mo supply in the future, including neutron irradiation from natural Mo, which offers a low radioactive waste and simple facilities without the use of ^{235}U. However, this production route possesses the main drawback, namely the low specific activity of resulting ^{99}Mo [3]. The consequence of this drawback is alumina no longer adequate as an adsorbent for ^{99}Mo/^{99m}Tc generator. A new material with higher Mo adsorption capacity is indispensable for further development of ^{99}Mo/^{99m}Tc generator [4–6].

In recent decades, mesoporous alumina (MA) has attracted the attention of the industrial and scientific fields due to its wide variety of applications. This material is widely used as a chemical catalyst/catalyst support [7], and sorbent [8]. Furthermore, it possesses potential applications in energy storage [9], sensing [10, 11], and biomedical application [12, 13]. MA possesses versatile functions because of its typical properties, such as high surface area, porosity, stability, and chemically active sites on its surface [14]. These unique properties of MA offer an application as an adsorbent in various fields, including the development of the ^{99}Mo/^{99m}Tc generator.

To date, MA has been developed as a Mo adsorbent using various types of synthesis routes. Chakravarty et al. [15] produced MA using glucose-template and evaluated its performance on high activity ^{99}Mo (26 GBq). In their work, double-column design played an essential role in the increase of the quality of eluates, namely ^{99}Mo breakthrough and percentage of yield. This study has opened the further work of the application of MA on ^{99}Mo/^{99m}Tc generator development. Chakravarty et al. [16] also developed MA

✉ Miftakul Munir
miftakul@batan.go.id

[1] Center for Radioisotope and Radiopharmaceutical Technology, National Nuclear Energy Agency of Indonesia (BATAN), Puspiptek Area, South Tangerang 15314, Indonesia

from the same template using a solid-state synthesis method, which offered a facile synthesis route without solvent. As a proof of concept, a radiolabelling process with clinical doses and the pre-clinical study was also conducted, which demonstrated a comparable result with that of radiopharmaceutical prepared from the commercial one. Saptiama et al. [8] developed MA using a soft-template approach, which revealed that the surface area and pore volume decrease as the calcination temperature increases. Saptiama and co-workers [17] also reported the development of MA using a template-free method with mere "water-ethanol" treatment, which demonstrated a better Mo adsorption capacity than the untreated one. The other study revealed the role of amino acids on multi-layered nano-sheets formation of MA with high surface area [18]. These synthesis pathways confer remarkable characteristics to the material and potential as Mo adsorbent. However, the sophisticated method and expensive starting material make it challenging to produce commercial MA and ^{99}Mo/^{99m}Tc generator at an affordable price.

In an attempt to develop a cost-efficient production method for MA, a waste-based synthesis route has been developed for a broad range of application. Besides reducing the cost of starting material, this MA production route lowered the number of various wastes, which harm the environment. Li et al. [19] developed well-shaped Al_2O_3 from an oil shale-ash waste using a urea-precipitation method with hard-templates. Even though it employed a simple process and produced hollow microspheres, an expensive chemical compound was required. Chotisuwan et al. [20] were able to develop an MA from aluminium cans as catalytic support for toluene oxidation. However, expensive chemicals were still used in the production process. A green synthesis method was developed by Yan et al. [21] for MA production from coal fly ash using a lime-sinter method with extraction efficiency up to 87.42% and surface area of 230.3 $m^2\ g^{-1}$. Osman and co-workers [22, 23] also produced MA from an aluminium foil waste using facile and green methods with a surface area up to 300 $m^2\ g^{-1}$. This study also revealed that MA produced from aluminium foil waste possesses better properties than MA produced from commercial aluminium chloride ($AlCl_3$). Having a high surface area and low chlorine content, the MA is suitable as an acid catalyst for dimethyl ether production from methanol. From these studies, it can be concluded that the waste-based MA production method promises an invaluable material with various applications, including as a cost-efficient adsorbent on ^{99}Mo/^{99m}Tc generator development.

In this work, for the first time, we utilised MA from aluminium foil waste as an adsorbent in the ^{99}Mo/^{99m}Tc generator system. The synthesis method was adapted from Osman et al. [22] with a slight modification to simplify the process. As a proof of concept, the ^{99}Mo adsorption and ^{99m}Tc releasing performance of MA was evaluated in a ^{99}Mo/^{99m}Tc generator system with a loading activity of 1.97–9.81 GBq (24–37 GBq g^{-1}). The quality of the ^{99m}Tc generated from the system was also evaluated to ascertain its obedience to compendia. Finally, as the very first step to head a clinical trial, radiolabelling of various radiopharmaceutical kits was performed. Three kits were selected to represent a simple and complex radiolabelling process, as well as a newly developed radiopharmaceutical.

Experimental

Chemicals

Aluminium foil waste was collected from the Center for Radioisotope and Radiopharmaceutical Technology, the National Nuclear Energy Agency (BATAN). Ammonia solution (NH_3) 32%, molybdenum trioxide (MoO_3), and acidic alumina were purchased from Sigma Aldrich, while hydrochloride acid 37% (HCl) and sodium hydroxide (NaOH) were obtained from Merck.

Material preparation

The material synthesis method was adapted from Osman et al. [22]. An adequate amount of aluminium foil waste was carefully dissolved in 6 M HCl solution and stored overnight. The solution was filtered to remove the impurities and then heated at 100 °C for 10 min. After that, 32% NH_3 solution was added dropwise until the precipitation is complete. The precipitate was then dried at 120 °C, and followed by calcination at 600 °C for 4 h. The dried precipitate and calcinated alumina are designated as GA FL120 and GA FL600, respectively.

Material characterisation

The morphology of GA FL120 and GA FL600 was characterised by using field-emission scanning electron microscopy using a FESEM Hitachi SU-8000 and transmission electron microscopy on JEOLJEM-1400 120 kV. Nitrogen adsorption-desorption analysis was performed using Quantachrome NovaWin, where the specific surface area and the pore size distribution were calculated by the Brunauer–Emmet–Teller (BET) and Barrett–Joyner–Halenda (BJH) method, respectively. The Fourier transform infrared (FTIR) analysis was performed using an Alpha FTIR Spectrometer Bruker at 4000–400 cm^{-1}. The phase composition was evaluated by X-ray diffraction (XRD) on Rigaku SmartLab 3 kW. Thermogravimetric analysis (TGA) and differential scanning calorimetry (DSC) were carried out using Setaram LabSys Evo S60/58998 under airflow from room temperature to 650 °C. The ^{99m}Tc radioactivity was measured using a

dose calibrator (Biodex Atoab 100 plus) whereas the ^{99}Mo breakthrough was evaluated using a multichannel analyzer (Ortec XCOOLER MCA) with Pb shield container designed to remove gamma emission of ^{99m}Tc.

^{99}Mo/^{99m}Tc generator development

The production of ^{99}Mo in a GA Siwabessy multipurpose reactor has been described elsewhere [2]. 5 g of GA FL600 was packed in the frit column with a dimension of 2 × 10 cm and then assembled in a ^{99}Mo/^{99m}Tc generator system.

An aliquot of ^{99}Mo with the activity of 1.97–9.81 GBq containing 0.05–0.27 g Mo was then added to the column followed by the measurement of ^{99}Mo activity of the filtrate. Subsequently, the column was rinsed with distilled water until the ^{99}Mo activity of the filtrate get near to the background, and was rinsed with saline solution to release ^{99m}Tc. After about 24 h, the column was eluted with a saline solution as 1 mL aliquots with or without a secondary column (dimension of 1 × 8 cm) as shown in Fig. 7, and the eluates were then measured for gamma activity using Dose Calibrator of AtomLab 100. The elution was carried out for three consecutive days to evaluate the robustness of the system.

Quality control of the ^{99m}Tc eluate was performed for its aluminium content, pH, radiochemical purity (RCP), and visual aspect using standard methods. The radiolabeling process of ^{99m}Tc-MDP, ^{99m}Tc-MIBI, and ^{99m}Tc-ethambutol have been described elsewhere [24, 25]. The RCP of the resulting ^{99m}Tc-radiopharmaceutical was analysed by thin-layer chromatography with stationary and mobile phase composition as described in Table 1.

Results and discussion

Synthesis of MA from aluminium waste

MA synthesis procedure has been widely developed to produce a variety of morphologies and structures. The application of MA on the ^{99}Mo/^{99m}Tc generator based on low specific activity ^{99}Mo has attracted the interest of researchers from all around the world. However, this type of ^{99}Mo/^{99m}Tc generator has not available commercially due to sophisticated synthesis procedures and expensive materials. This work offers a promising facile method to produce MA as an adsorbent for ^{99}Mo/^{99m}Tc generator. A facile and green MA synthesis method from aluminium waste developed by Osman et al. has been adopted in this work. The MA synthesis can be divided into three main steps, synthesis of $AlCl_3$, the formation of AlOOH or boehmite, and the development of Al_2O_3. $AlCl_3$ was produced by the rapid dissolving of aluminium foil waste in HCl solution. The second step is very important because, without a template, AlOOH structure or composition is the only determinant prior to the calcination process. The critical parameter in this step is the NH_3 addition, which hydrolyses $AlCl_3$ and forms AlOOH. The last step was the calcination process, which liberates water and other compounds during Al_2O_3 formation. A template or directing agent was not employed to understand the characteristic of Al_2O_3 produced from mere $AlCl_3$ from precipitation.

The resulting MA from this work was yellowish and formed a big lump, which became small granular after grinding. The synthesis yield was more than 80%, and the largest batch was ~ 10 g. The MA was kept in a sealed container prior to analysis and further study.

Table 1 Stationary and mobile phase composition for RCP evaluation of ^{99m}Tc-radiopharmaceutical

Radiopharmaceutical	Stationary phase	Mobile phase
^{99m}Tc–MDP	1. Whatman paper 2. Whatman paper	1. Methyl ethyl ketone 2. Saline solution
^{99m}Tc–MIBI	Alumina TLC	Ethanol
^{99m}Tc–ethambutol	1. Silica gel 2. Whatman 31ET	1. Acetone 2. Acetonitrile:water (1:1)

Morphology and characterisation

The SEM image of GA FL120 and GA FL600 is shown in Fig. 1a, b, respectively. It shows that GA FL120, which is boehmite, formed small and compact particles, while GA FL600 formed a big and solid cluster showing irregular craters on the surface. This compact structure was formed due to the absence of a template or surfactant, an essential factor in the morphology development of material [26]. These directing agents are usually employed in MA synthesis to generate a unique structure of MA. However, this study was performed without the directing agent to understand the nature of MA produced from aluminium waste. In the absence of these "building blocks", boehmite merely forms anhedral laths, which transform to compact structures during calcination [27]. A compact and solid structure is required for separating material, especially for radioisotope separation, because the radiation emission might influence the chemical structure and attenuate the physical strength of the material. The presence of excessive cracks or small particles in a material may interfere with the elution process in the column generator. After several times of elution, the generator column can be clogged. The TEM images, as shown in Fig. 2a, b reveal that GA FL600 consists of a small amount of nano-sphere and excessive irregular agglomeration. The TEM images also reveal that the GA FL600 contains pores with a diameter of < 50 µm, which is in agreement with the results obtained from BET and BJH methods (Fig. 3).

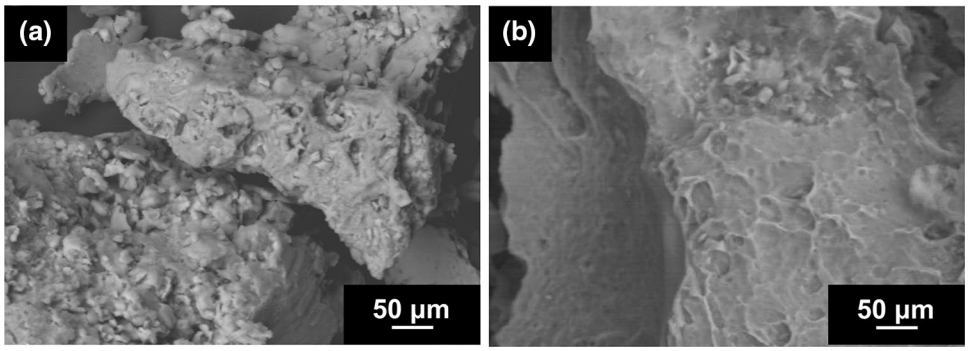

Fig. 1 SEM images of GA FL120 (**a**) and GA FL600 (**b**).

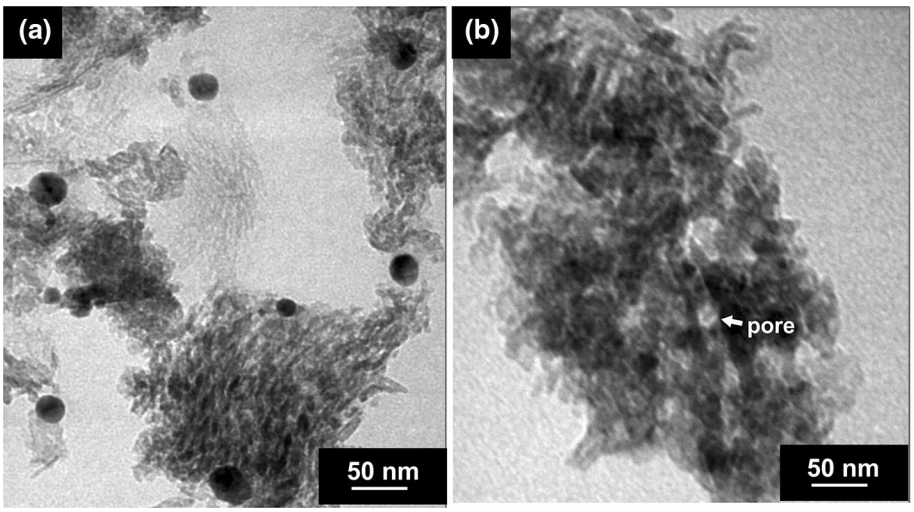

Fig. 2 Low and high magnification TEM images of GA FL600 (**a**) and (**b**), respectively.

Table 2 Surface area (S_{BET}), pore volume pore diameter, and % mass of Chlor (Cl) for alumina derived from aluminium foil waste both GA FL120 and GA FL600.

Material	S_{BET} ($m^2\ g^{-1}$)	Pore volume ($cm^3\ g^{-1}$)	Pore diameter (nm)	EDX (% Cl mass)
GA FL120	173.6	0.25	1.71	25.6
GA FL600	209.8	0.49	4.56	0.80

The EDX data shown in Table 2 reveals that % Cl in GA FL120 is far higher than that of GA FL600, with 25.8% and 0.8% respectively. It is obvious that the calcination process reduces the chlorine content, even though the non-negligible amount of this element remains. The presence of chlorine in alumina can deactivate its catalytic ability [23]. However, it is unclear whether chlorine can interfere with the adsorption capacity or not. After all, alumina prepared from aluminium waste contains a lower chlorine content (1.8%) compared to the commercial one (3.8%), and Osman et al. proved that MA containing 1.8% chlorine demonstrated an excellent catalytic performance [22]. Therefore, the ^{99}Mo performance of the MA produced in this work should not be interfered with by lower chlorine content. The EDX data also reveal that GA FL600 contains an undetectable amount of nitrogen, which exists prior to calcination. It is favourable because the presence of nitrogen may influence the ^{99}Mo adsorption and an eluate quality.

As shown in Table 2, the surface area of GA FL120 is slightly lower than GA FL600, while its pore volume and pore diameter are half of GA FL600. The high-temperature calcination process is associated with the opening of a porous network and channel arrangement due to water evaporation and the removal of other species during decomposition [18]. Furthermore, the calcination process changes the material from microporous (GA FL120) to mesoporous (GA FL600).

The N_2 adsorption-desorption isotherms and pore size distribution are presented in Fig. 3, which demonstrates type IV isotherm with H2 slightly shifting to H3 type hysteresis loops. This finding reveals that GA FL600 is a mesoporous material with ink-bottle connectivity, a capillary condensation phenomenon and relatively narrow pore size distribution [14, 28]. This work proves that MA can still be prepared conventionally without surfactant or template because the pores were naturally formed from inter-particle stacking from primary and secondary precursors [29]. The relatively narrow pores distribution is also demonstrated by the pore

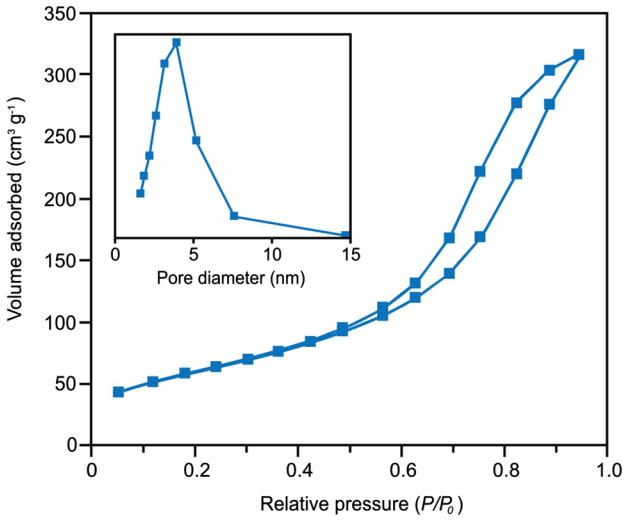

Fig. 3 N_2 adsorption-desorption isotherms, and pore-size distribution plot of the GA FL600.

diameter diagram. It is worth noting that the conventional synthesis of MA is able to produce narrow pore distribution.

A comparison of the FT-IR spectra of GA FL600 and GA FL120 is presented in Fig. 4. The FT-IR spectra show profoundly different spectra as a consequence of the calcination process. In the spectra of GA FL120, the broad peak at 3250–3500 cm^{-1} is related to the O–H stretching vibration and physically adsorbed water on the surface; the other medium peak at 1631 cm^{-1} is related to the H-OH scissor mode of adsorbed water [30, 31]. The peak at 3250 cm^{-1} reflects the stretching vibration of N–H from the excessed ammonia, and the reacted ammonia can be identified from the appearance of 1500 cm^{-1} peak due to N–O stretching. Moreover, the peaks around 1072 cm^{-1} and 487 cm^{-1} are attributed to Al–O–H symmetric bending and the angle bending of (OH)-Al=O, respectively [32, 33]. In the spectra of GA FL600, most of the peaks disappear, leaving the broad extending peak in the range 400–700 cm^{-1}, which is the signature of γ-Al_2O_3 with the presence of amorphous structure as correlated with the XRD pattern presented in Fig. 5 [33].

Figure 5 shows the XRD pattern of GA FL120, which corresponds to pseudo-boehmite with low crystallinity and a significant quantity of NH_4Cl (PDF No. 7-0007). This occurs due to the low solubility of NH_4Cl, although the material had been washed with distilled water after precipitation [34]. The diffractogram of GA FL600 displays the diffraction line, which corresponds to γ-Al_2O_3 (JCPDS Card No. 00-010-0425) with poor crystallinity indicated by the weak intensity [17]. From the XRD pattern of GA FL120 and GA FL600, it can be concluded that pseudo-boehmite can be produced from aluminium foil waste followed by γ-Al_2O_3 formation after calcination at 600ºC.

The γ-Al_2O_3 formation from aluminium waste was confirmed by TG-DSC at the ambient atmosphere as presented in Fig. 6. The weight loss percentage from the thermogravimetry is 74.3%, which is comparable to the theoretical value of 78.8% calculated by Eq. 1.

$$2AlCl_3 \cdot 6H_2O \rightarrow Al_2O_3 + 6HCl + 9H_2O \quad (1)$$

The weight loss process can be separated into three main steps, as shown in Fig. 6. The first step occurs below 200 ºC as a consequence of the evaporation of physically adsorbed water [27]. The second step in the temperature range of 200–350 ºC with a weight loss of 59.7% is correlated to the first step dehydroxylation of boehmite to form γ-Al_2O_3 [35, 36]. The excessive weight loss more than the theoretical γ-Al_2O_3 formation of 15% is caused by the removal of nitrogen and chlorine species. The last step above 350 ºC is attributed to the further dehydroxylation process [37]

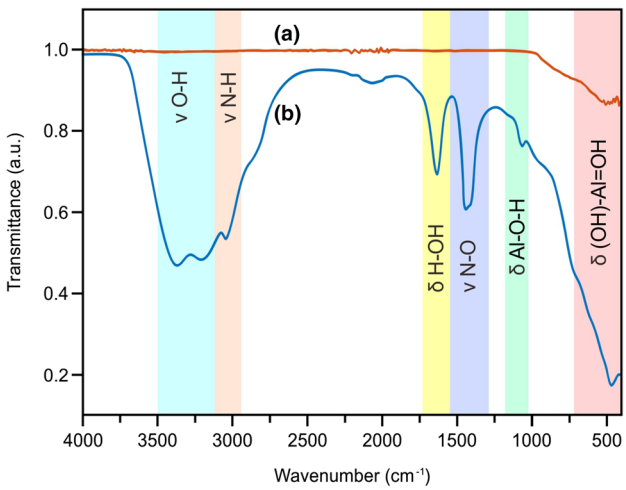

Fig. 4 FT-IR spectra of GA FL600 (**a**) and GA FL120 (**b**).

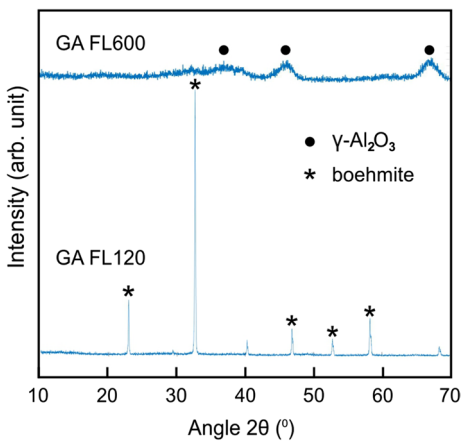

Fig. 5 XRD patterns of the GA FL120 and GA FL600.

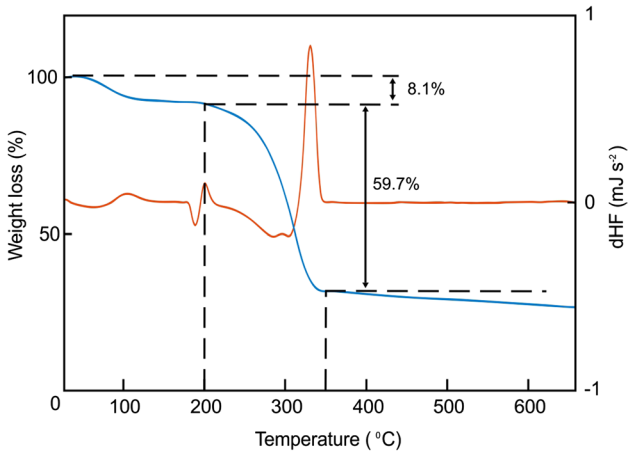

Fig. 6 Thermogravimetry and differential scanning calorimetry of alumina prepared from aluminium foil waste.

^{99}Mo/^{99m}Tc generator

^{99}Mo production

The low specific activity of ^{99}Mo for this experiment was produced by neutron irradiation of natural Mo with ^{98}Mo content of 24.13%. The irradiation time in a GA Siwabessy multipurpose reactor was ~ 100 h with a maximum neutron flux of approximately 2.5×10^{14} n cm^{-2} s^{-1} [38]. In one typical production period with 4 g of MoO_3, ~ 55.5 GBq (1500 mCi) of ^{99}Mo was obtained with a specific activity of ~ 13.875 GBq (375 mCi) per gram of Mo. The obtained powder of MoO_3 was dissolved in 4M NaOH at room temperature to get a colourless solution.

The advantages of ^{99}Mo obtained from neutron-irradiated MoO_3 is the simple post-irradiation process and its high radionuclide purity. The post-irradiation processes prior to generator assembly are mere simple dissolving process and purity analysis using gamma spectroscopy. The post-irradiation process for ^{99}Mo prepared from ^{235}U is very complicated because there are numerous fission products with a very long half-life. The other issue with ^{99}Mo prepared from fission products is the high activity of radioactive waste with more than hundreds of years half-life. However, the specific activity of ^{99}Mo prepared from natural MoO_3 is very low compared to the fission ^{99}Mo, because it is not carrier-free. There is a huge amount of non-irradiated molybdenum in the low specific activity ^{99}Mo solution.

^{99}Mo/^{99m}Tc separation

To develop a ^{99}Mo/^{99m}Tc separation system with high elution efficiency and good quality, three generator models were prepared, as presented in Fig. 7: (1) single-column system using GA FL600 as ^{99}Mo sorbent; (2) double-column system GA FL600 as ^{99}Mo sorbent and ^{99}Mo breakthrough trap; (3) double-column system using GA FL600 as ^{99}Mo sorbent and acidic alumina as ^{99}Mo breakthrough trap. It is obvious that the double-column system will perform better results [15]. However, the single column is reported to understand the nature of alumina derived from aluminium waste in the ^{99}Mo/^{99m}Tc separation system.

A low specific activity ^{99}Mo of 1.97–9.81 GBq was loaded to the column with ^{99}Mo adsorption result of 60.2 ± 1.5 mg Mo/g of the sorbent. The ^{99m}Tc elution from three separation models was displayed in Fig. 7, which demonstrated different profiles, as shown in Fig. 8. The single-column system exhibits a broad profile with the highest yield in the second elution. A similar profile is also demonstrated

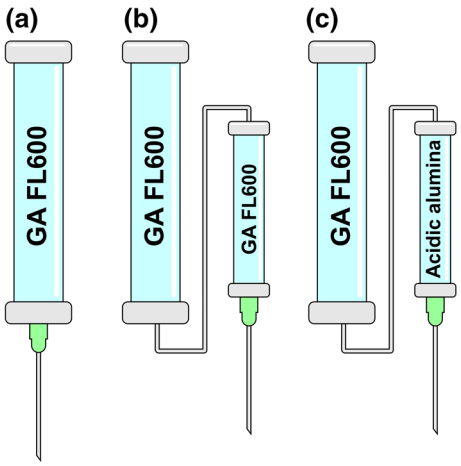

Fig. 7 ^{99}Mo/^{99m}Tc separation system using a single column (**a**), GA FL600 double-column (**b**), and GA FL600–acidic alumina double-column (**c**)

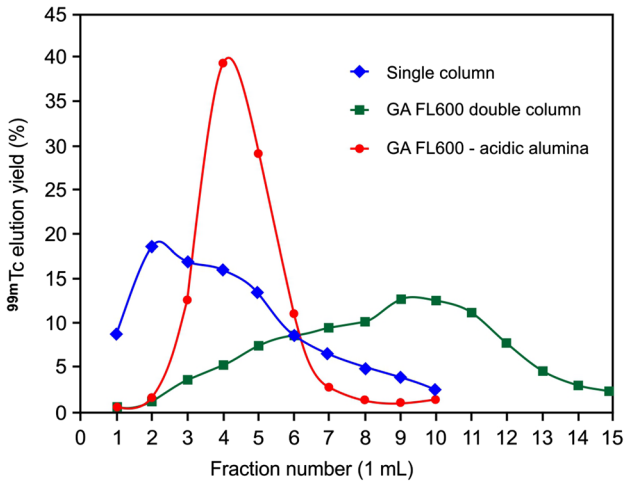

Fig. 8 ^{99m}Tc elution profile of single column, GA FL600 double-column, and GA FL600–acidic alumina double-column.

by GA FL600 double-column with lower elution yield in each fraction and more than ten fractions.

In contrast, GA FL600–acidic alumina double-column exhibits a reasonably sharp peak with the highest in the fourth fraction. It can be concluded that acidic alumina tandem improves the elution profile generating a reasonably sharp peak [15]. Even though GA FL600 demonstrates higher adsorption capacity than acidic alumina, its ability to release ^{99m}Tc is lower than that of acidic alumina. The mechanism behind this phenomenon is unclear. The acidic alumina column might slightly adsorb the ^{99m}Tc released from the first column. Therefore, it can be a directing agent which makes the ^{99m}Tc eluted in the narrow range of volume resulting in higher concentration eluate. It is worth noting that this concentrated ^{99m}Tc is a prerequisite for radiolabeling practice in a hospital. It is obvious that the assembly process of a double-column generator is more complicated than that of the single column. However, no obstacle during elution was observed [15].

Further elution in three days, as presented in Table 3, was conducted to evaluate the performance of the generators for the influence of time. The adsorbed ^{99}Mo was the loaded ^{99}Mo subtracted by the ^{99}Mo activity in the rinsing water, while the elution yield was calculated as a ratio between the measured ^{99m}Tc activity and theoretical ^{99m}Tc activity. The optimum time of growth of ^{99m}Tc is around 24 h based on transient equilibrium [39]. The single column and GA FL600 generator demonstrate a high ^{99m}Tc elution yield of more than 100%, which reveals that the eluate contains ^{99}Mo. The activity of ^{99}Mo breakthrough is higher than the required standard from European Pharmacopeia (Ph.Eur) of 0.1% ^{99}Mo activity/^{99m}Tc activity. It is obvious that the single-column generator will release a significant amount of ^{99}Mo without a second column which is able to trap the breakthrough. In the GA FL600 double-column, the ^{99}Mo breakthrough is lower than in the single column, even though it still higher than the required standard.

In contrast, the GA FL600–acidic alumina double-column demonstrates a slightly lower ^{99m}Tc elution yield, while the ^{99}Mo breakthrough is the lowest. It can be concluded that the ability of acidic alumina on trapping ^{99}Mo breakthrough is better than GA FL600's. In an acidic environment pH of 3–4, the GA FL600 is better ^{99}Mo sorbent due to the higher surface area [17], however, in the higher pH, the acidic alumina possesses higher adsorption capacity due to its acidic properties.

Quality control of eluate

Quality assurance of eluate from ^{99}Mo/^{99}Tc generator is a critical factor since the eluate is used as parenteral preparation which might cause a severe effect on the patient in case the required standard is ignored [40]. In this early development of ^{99}Mo/^{99}Tc generator, the controlled quality aspects are ^{99}Mo breakthrough, aluminium content, pH, radiochemical purity, and visual aspect. The ^{99}Mo breakthrough has been described previously with variation results depend on the column models.

The presence of aluminium ion in ^{99}Tc eluate might interfere with the radiolabelling process resulting in false uptake in diagnosis. For instance, a lung uptake can be observed in bone scan with the presence of aluminium ion. Since aluminium might exist in the eluate because it washed by saline solution, an aluminium assay is highly essential. An aluminium breakthrough kit is a semi-quantitative method using the observation of colour change due to aluminium complex formation. The 10 μg ml^{-1} aluminium solution is used as a standard for colour comparison on the breakthrough assay. The breakthrough assay reveals that the aluminium content is below 10 μg ml^{-1}, which obeys the compendia. The pH of the eluate was 5.5, with an acceptable value based on Ph.Eur.

Table 3 Elution performances of (a) single column, (b) GA FL600 double-column, and (c) GA FL600–acidic alumina double-column

Day	Adsorbed ^{99}Mo activity (GBq)	Growth time (h)	Eluted ^{99m}Tc (GBq)	Elution yield (%)	^{99}Mo breakthrough (%)
(a)					
1	0.28	22.7	0.20	106.2	1.70
2	0.22	23.8	0.15	100.6	0.64
3	0.17	23.8	0.16	135.1	0.68
(b)					
1	4.85	19.3	3.50	107.8	0.00
2	3.96	21.0	3.03	113.5	0.46
3	3.15	23.1	1.09	108.7	0.75
(c)					
1	4.83	18.8	2.87	88.8	0.02
2	3.97	22.28	2.47	92.1	0.00
3	3.14	24.50	0.75	85.7	0.04

of 4.0–8.0. The pH of the eluate is slightly acidic because the acidity of MA might affect the saline solution.

The radiochemical purity (RCP) was conducted using thin-layer chromatography (TLC) with Whatman paper no.1 and 85% methanol in water as stationary and mobile phase, respectively. This assay is aimed to measure the TcO^{4-} compared to another species or radionuclide. The RCP of ^{99m}Tc for the GA FL600–acidic alumina was found to be ≥ 98%; the other columns demonstrate RCP of < 98%. The higher ^{99}Mo breakthrough might play an important role in the decrease of the RCP. Another species of technetium, such as Tc_2O, is rarely observed because it is laboriously eluted by saline solution. The visual inspection revealed that the eluate was clear, colourless, and not contain any particulate.

Radiolabelling

In order to simplify the use of radiopharmaceutical in hospitals, a pharmaceutical "cold" kit and radionuclide generator are prepared separately. The hospital can store a lot of "cold" kits for a long time because the half-life can be more than a year. A radionuclide generator with a shorter half-life can be purchased if demanded, and a simple radiolabelling process can be performed in the hospital. ^{99m}Tc-based "cold" kit is the most widely used diagnosis agent in the hospital.

^{99m}Tc is a unique radionuclide due to its ability to establish a complex with various ligands. The radiolabelling procedure is vary depending on the characteristic of the complex and ligand. The radiolabelling process is highly important for assessing the quality of the ^{99m}Tc eluate because the presence of impurity might easily affect the radiolabelling results. This process was conducted merely using the eluate from GA FL600–acidic alumina double-column due to its radiochemical and radionuclide purities. The radiopharmaceutical kits used for the radiolabelling were MIBI, MDP, and ethambutol. These kits contain a reducing agent, namely $SnCl_2$, for TcO_2 formation from TcO_4^-, which is able to form a complex with radiopharmaceutical ligand [41]. MIBI and MDP are commercially available kits. MIBI is well known as a cardiac imaging agent, which is the representation of a laboriously radiolabelled kit, while MDP, a bone scan agent, is an easily radiolabeled kit. The radiolabelling of MDP is conducted at room temperature, while the MIBI requires a high-temperature.

The quality of the radiolabelled kit was examined using a thin-layer chromatography method, which is a simple and inexpensive method. ^{99m}Tc–MDP was examined using two mobile phases, as shown in Table 1. Methyl ethyl ketone was used to evaluate the presence of free $^{99m}TcO_4^-$, while a saline solution was used to assess the impurity of $^{99m}TcO_2$ colloids. The evaluation ^{99m}Tc–MIBI was evaluated merely using alumina–ethanol system, which shows ^{99m}Tc–MIBI peak at Rf of 0.8–1. ^{99m}Tc–ethambutol was evaluated using two TLC systems, the first one was aimed to determine the $^{99m}TcO_4^-$ impurity, whole the second one was aimed to determine the $^{99m}TcO_2$ colloids impurity.

Radiolabelled results of MIBI, MDP, and ethambutol kits were 99.12, 98.76, and 88.82%, respectively. The RCP limit of ^{99m}Tc-MIBI and ^{99m}Tc-MDP based on USP are > 90% and > 95%, respectively [24]. Ethambutol kit is clinical phase ^{99m}Tc radiopharmaceutical, and there is no guidance for its RCP limit, however, based on the research experience, the expected RCP varies from 85 to 98% [25, 42].

All data presented here unveil the potential of MA prepared from aluminium foil waste as an adsorbent on a commercial ^{99}Mo/^{99m}Tc generator. The further pre-clinical study is required to understand the bio-distribution of the radiopharmaceuticals labelled by the ^{99m}Tc produced from this material-based ^{99}Mo/^{99m}Tc generator.

Conclusions

In this work, MA has been successfully produced from aluminium foil waste by using a facile and green method. Even though MA prepared from aluminium foil is not able to exhibit a better morphology, such as higher surface area, this material demonstrates a higher Mo adsorption capacity and ability to release ^{99m}Tc with a reasonable elution profile. The quality control of the resulting ^{99m}Tc eluate met the required standard. The radiolabelling process in three different kits also exhibited the ability of radiolabelling for various types of radiopharmaceutical kits. Furthermore, this work has opened a window for the development of remarkable sorbent material, especially as a ^{99}Mo sorbent, from aluminium waste. Further work can be arranged to improve the MA properties by using a directing agent or another sophisticated method. A pre-clinical and clinical trial is also required prior to the commercial application of ^{99}Mo/^{99m}Tc generator based on alumina from aluminium foil waste.

Acknowledgements The authors acknowledge the Ministry of Research Technology and Higher Education of Indonesia for its financial support through INSINAS programme (project number: 06/INS-1/PPK-E4/2019.

Compliance with ethical standards

Conflict of interest The authors declare that they have no conflict of interest.

References

1. van Wyngaardt WM, Tobin SM, Lee S et al (2020) Primary standardisation of technetium-99m by liquid scintillation coincidence counting. Appl Radiat Isot 156:108935
2. Saptiama I, Lestari E, Sarmini E et al (2016) Development of ^{99}Mo/^{99m}Tc generator system for production of medical

radionuclide ^{99m}Tc using a neutron-activated ^{99}Mo and zirconium based material (ZBM) as its adsorbent. Atom Indones 42:115–121
3. Blaauw M, Ridikas D, Baytelesov S et al (2017) Estimation of ^{99}Mo production rates from natural molybdenum in research reactors. J Radioanal Nucl Chem 311:409–418
4. Mostafa M, Atef M, El-Amir MA (2017) Preparation and performance studies of ^{99}Mo/^{99m}Tc column generators based on nano zirconium molybdate. J Radioanal Nucl Chem 314:1683–1694
5. Chattopadhyay S, Das SS, Alam MN et al (2017) Preparation of ^{99}Mo/^{99m}Tc generator based on cross-linked chitosan polymer using low-specific activity (n,γ)^{99}Mo. J Radioanal Nucl Chem 313:647–653
6. Chattopadhyay S, Saha Das S, Barua L et al (2019) A compact solvent extraction based ^{99}Mo/^{99m}Tc generator for hospital radiopharmacy. Appl Radiat Isot 143:41–46
7. Zhang ZS, Fu XP, Wang WW et al (2018) Promoted porous Co_3O_4–Al_2O_3 catalysts for ammonia decomposition. Sci China Chem 61:1389–1398
8. Saptiama I, Kaneti YV, Suzuki Y et al (2017) Mesoporous alumina as an effective adsorbent for molybdenum (Mo) toward instant production of radioisotope for medical use. Bull Chem Soc Jpn 90:1174–1179
9. Kaneti YV, Salunkhe RR, Wulan Septiani NL et al (2018) General template-free strategy for fabricating mesoporous two-dimensional mixed oxide nanosheets via self-deconstruction/reconstruction of monodispersed metal glycerate nanospheres. J Mater Chem A 6:5971–5983
10. Pandey M, Mishra P, Saha D et al (2014) Development of commercial trace moisture sensor: a detailed comparative study on microstructural and impedance measurements of two phases of alumina. Electron Mater Lett 10:357–362
11. Laatar F, Harizi A, Zarroug A et al (2017) Novel CdSe nanorods/porous anodic alumina nanocomposite-based ethanol sensor: sensitivity enhancement by visible light illumination. J Mater Sci Mater Electron 28:12259–12267
12. Vignesh Raj S, Rajkumar M, Meenakshi SN et al (2018) Synthesis and characterisation of hydroxyapatite/alumina ceramic nanocomposites for biomedical applications. Bull Mater Sci 41:93
13. Rahmati M, Mozafari M (2019) Biocompatibility of alumina-based biomaterials—a review. J Cell Physiol 234:3321–3335
14. Mahinroosta M, Allahverdi A, Dong P et al (2019) Green template-free synthesis and characterisation of mesoporous alumina as a high value-added product in aluminum black dross recycling strategy. J Alloys Compd 792:161–169
15. Chakravarty R, Ram R, Mishra R et al (2013) Mesoporous alumina (MA) based double-column approach for development of a clinical scale ^{99}Mo/^{99m}Tc generator using (n,γ) ^{99}Mo: an enticing application of nanomaterial. Ind Eng Chem Res 52:11673–11684
16. Chakravarty R, Bahadur J, Lohar S et al (2019) Solid state synthesis of mesoporous alumina: a viable strategy for preparation of an advanced nanosorbent for ^{99}Mo/^{99m}Tc generator technology. Microporous Mesoporous Mater 287:271–279
17. Saptiama I, Kaneti YV, Suzuki Y et al (2018) Template-free fabrication of mesoporous alumina nanospheres using post-synthesis water-ethanol treatment of monodispersed aluminium glycerate nanospheres for molybdenum adsorption. Small 14:1800474
18. Saptiama I, Kaneti YV, Yuliarto B et al (2019) Biomolecule-assisted synthesis of hierarchical multilayered boehmite and alumina nanosheets for enhanced molybdenum adsorption. Chem A Eur J 25:4843–4855
19. Li G, Wang W, Long T et al (2014) A general and facile method to prepare uniform gamma-alumina hollow microspheres from waste oil shale ash. Mater Lett 133:143–146
20. Chotisuwan S, Sirirak A, Har-Wae P et al (2012) Mesoporous alumina prepared from waste aluminum cans and used as catalytic support for toluene oxidation. Mater Lett 70:125–127
21. Yan F, Jiang J, Liu N et al (2018) Green synthesis of mesoporous γ-Al_2O_3 from coal fly ash with simultaneous on-site utilization of CO_2. J Hazard Mater 359:535–543
22. Osman AI, Abu-Dahrieh JK, McLaren M et al (2017) A facile green synthetic route for the preparation of highly active γ-Al_2O_3 from aluminum foil waste. Sci Rep 7:3593
23. Osman AI, Abu-Dahrieh JK, Laffir F et al (2016) A bimetallic catalyst on a dual component support for low temperature total methane oxidation. Appl Catal B Environ 187:408–418
24. Valenzuela G, Környei J, Mikolajczak M et al (2008) Technetium-99m radiopharmaceuticals: manufacture of kits. IAEA, Vienna
25. Shah SQ, Ullah N (2019) Pre-clinical evaluation of ^{99m}Tc-ethambutol, an alternative tuberculosis diagnostic tool. Radiochemistry 61:233–237
26. Xu N, Liu Z, Dong Y et al (2016) Controllable synthesis of mesoporous alumina with large surface area for high and fast fluoride removal. Ceram Int 42:15253–15260
27. Wu W, Wan Z, Chen W et al (2015) Synthesis of mesoporous alumina with tunable structural properties. Microporous Mesoporous Mater 217:12–20
28. Afshar Taromi A, Kaliaguine S (2017) Synthesis of ordered mesoporous γ-alumina – Effects of calcination conditions and polymeric template concentration. Microporous Mesoporous Mater 248:179–191
29. Yacob AR, Bello AM, Kabo KS (2016) The effect of polyoxyethylene (40) stearate surfactant on novel synthesis of mesoporous γ-alumina from Kano kaolin. Arab J Chem 9:297–304
30. Copeland JR, Santillan IA, Schimming SM et al (2013) Surface interactions of glycerol with acidic and basic metal oxides. J Phys Chem C 117:21413–21425
31. Cai W, Tan L, Yu J et al (2014) Synthesis of amino-functionalized mesoporous alumina with enhanced affinity towards Cr(VI) and CO_2. Chem Eng J 239:207–215
32. Zhang L, Jiao X, Chen D et al (2011) γ-AlOOH nanomaterials with regular shapes: Hydrothermal fabrication and $Cr_2O_7^{2-}$ adsorption. Eur J Inorg Chem 2011:5258–5264
33. Djebaili K, Mekhalif Z, Boumaza A et al (2015) XPS, FTIR, EDX, and XRD analysis of Al_2O_3 scales grown on PM2000 alloy. J Spectrosc 2015:1–16
34. Temuujin J, Jadambaa T, Mackenzie KJD et al (2000) Thermal formation of corundum from aluminium hydroxides prepared from various aluminium salts. Bull Mater Sci 23:301–304
35. Yang Q (2011) Synthesis of γ-Al_2O_3 nanowires through a boehmite precursor route. Bull Mater Sci 34:239–244
36. Alex TC (2014) An insight into the changes in the thermal analysis curves of boehmite with mechanical activation. J Therm Anal Calorim 117:163–171
37. Huang H, Wang L, Cai Y et al (2015) Facile fabrication of urchin-like hollow boehmite and alumina microspheres with a hierarchical structure via Triton X-100 assisted hydrothermal synthesis. CrystEngComm 17:1318–1325
38. Liem PH, Tran HN, Sembiring TM (2015) Design optimization of a new homogeneous reactor for medical radioisotope Mo-99/Tc-99m production. Prog Nucl Energy 82:191–196
39. Uccelli L, Boschi A, Pasquali M et al (2013) Influence of the generator in-growth time on the final radiochemical purity and stability of radiopharmaceuticals. Sci Technol Nucl Install 2013:1–7
40. Maioli C, Lucignani G, Strinchini A et al (2017) Quality control on radiochemical purity in technetium-99m radiopharmaceuticals

labelling : three years of experience on 2280 procedures. Acta Biomed 88:49–56
41. Papagiannopoulou D (2017) Technetium-99m radiochemistry for pharmaceutical applications. J Label Compd Radiopharm 60:502–520
42. Singh N, Bhatnagar A (2010) Clinical evaluation of efficacy of 99mTc-ethambutol in tubercular lesion imaging. Tuberc Res Treat 2010:1–9